The Egyptian Journal of Radiology and Nuclear Medicine 47 (2016) 1575–1584

Contents lists available at ScienceDirect

The Egyptian Journal of Radiology and Nuclear Medicine

journal homepage: www.sciencedirect.com/locate/ejrnm

Original Article

Diffusion-Weighted MRI and apparent diffusion coefficient value in assessment of intra-medullary spinal cord masses

Doaa Ibrahim Hasan [a,*], Mohamed H. Abowarda [b], Mahmoud M. Taha [c]

[a] Diagnostic Radiology Department, Zagazig University, Egypt
[b] Radiology Department, Zagazig University, Egypt
[c] Neuro-surgery Department, Zagazig University, Egypt

ARTICLE INFO

Article history:
Received 22 May 2016
Accepted 15 June 2016
Available online 18 July 2016

Keywords:
Diffusion weighted imaging
Magnetic resonance imaging
Intramedullary spinal cord masses
Apparent diffusion coefficient

ABSTRACT

The purpose of this study was to evaluate use of Diffusion-Weighted MRI (DWI) and apparent diffusion coefficient value (ADC) in differentiation of intra-medullary spinal cord masses (IMSCM). Patients and methods: This study was carried out during the period from June 2013 to January 2016. It included 66 adult consecutive patients with intra-medullary SC masses. Results: The patients mean age was 45.48 ± 15.9 (18–72 y). Histopathological classification to benign/low grade malignancy group was in 53 patients and high grade malignancy group in 13 patients. No statistically significant difference between both groups regarding the patient age or their clinical presentation. There was a statistically significant difference between the two groups regarding the tumor location and enhancement pattern. There was statistically significant difference between the benign/low grade IMSC masses and high grade IMSC tumors ($p < 0.001$). Calculated mean ADC values in the benign/low grade tumors were high (1.26×10^{-3} mm^2/sec) compared to high grade tumors which were $0.89 \pm 0.40 \times 10^{-3}$ mm^2/sec. Conclusion: DWI and ADC values may be useful in providing information about tumors grading not available with conventional MR imaging in the evaluation of IMSC masses.

1. Introduction

MRI is the technique of choice for the spinal cord imaging because of a high sensitivity for different pathologic intramedullary changes [1]. Diffusion-Weighted MRI (DWI) promises to supply further information because of characteristic changes of the apparent diffusion coefficient (ADC), such as those manifested in acute ischemia, tumors, or lesions associated with multiple sclerosis [2,3].

The WHO classification also provides a grading system for tumors of each cell type and allows the classification of tumors to guide the choice of therapy and predict prognosis [4,5].

The most common kinds of intramedullary tumors are ependymomas, astrocytomas, and hemangioblastomas. In adults, ependymomas are the most common tumor type, accounting for 40–60% of all intramedullary spinal tumors. In children, astrocytomas are the most common tumor type, accounting for around 60% of all intramedullary spinal tumors [6,7]. However surgical resection is most effective at reducing disease burden, but carries significant risks of morbidity. Differentiating nature of these lesions and discretely marginated from infiltrating tumors is important for surgical planning [8]. The purpose of this

Peer review under responsibility of The Egyptian Society of Radiology and Nuclear Medicine.

* Corresponding author.
E-mail address: dididodge13@gmail.com (D.I. Hasan).

http://dx.doi.org/10.1016/j.ejrnm.2016.06.010
0378-603X/

study was to evaluate use of Diffusion-Weighted MRI imaging and apparent diffusion coefficient value in differentiation of intra-medullary spinal cord masses.

2. Patients and methods

This study was carried out in Radiodiagnosis Department, Zagazig University Hospitals during the period from June 2013 to January 2016. This study included 66 adult consecutive patients (39 men and 27 women) with intramedullary SOL; five children with intramedullary spinal cord tumor (IMSCT) were excluded from this study. The patients ranged in age from 18 to 79 years (mean 44.6 years). They were referred from Neurology and Neurosurgery Departments. The study was approved by our hospital institutional review board and an informed consent was obtained from each patient before participating in the study.

Inclusion criteria: Adult age group and any sex. Patients with IMSC masses proved by conventional T1 and T2 MRI.

Exclusion criteria: Patients unwilling to complete the study, extramedullary lesions and abnormal intramedullary signal intensity.

3. Patients were subjected to the following:

1- Clinical assessment.
2- Imaging.

- Conventional MR using Philips MR machine (Achieva – class II, 01.5 T).
  - Sagittal and axial T1WIs (pre and post-contrast) and T2WIs were acquired with a 4-mm section thickness, 380-mm field of view, 258 × 512 matrix, and the following sequences: T1-weighted spin echo (SE) (600/12 [repetition time TR msec/echo time TE msec]) and T2-weighted SE (5000/120 TR/TE). Post contrast sag. T1 after Magnevist [Gadolinium-("Gd-DTPA")], it was administrated IV in a dose of 0.1 mmol/kg body weight (0.2 ml/kg).
  - Axial T1 W and T2 W images were acquired with 4-mm section thickness, 380-mm field of view, 192 × 256 matrix.

Diffusion MRI:

- Fast scout scans in sagittal and axial planes were obtained and with image guidance, the volume of interest was positioned within each lesion, carefully excluding other structures.
- DW-MRI was obtained using a multi-section single shot spin echo EPI sequence with diffusion sensitivities of *b* values = 0 and 1000 s/mm^2.
- The diffusion gradient was applied sequentially in the three orthogonal directions (TR/TE: 1600/95 ms), and matrix (176 × 256), thickness (6 mm), gap (1 mm), Fov (40 × 20), acquisition time [4], and a standard phased array surface receiver coil for imaging the spine was used.
- ADC maps were formed automatically by the device, and circular regions of interest (ROIs) approximately 10 mm in diameter were placed in the center of the lesion to obtain ADC value with *b* values 1000 s/mm^2.

Blinded to histopathological information we evaluated the MRI images regarding the tumor size, locations, margin, signal intensity (SI) of the solid or cystic components of the tumor on T2-weighted and T1-weighted images, pattern of enhancement, and the presence of syringohydromyelia, tumoural cyst, non-tumoural cyst, hemorrhage, and cap sign, signal intensity of the SC masses in DWIs at *b*

Table 1
Comparison between benign/borderline tumors and malignant tumors as regards demographic and clinical data.

Demographic and clinical data	All patients (*N* = 66)	Benign/low grade malignancies (*N* = 53)	High grade/malignancies (*N* = 13)	*p*-value
Age				
Mean ± SD	45.48 ± 15.90	44.49 ± 15.65	49.53 ± 16.90	0.242[a]
Median (range)	47 (18–72)	46 (18–72)	52 (23–71)	
⩽20 years	3 (4.5%)	3 (5.7%)	0 (0%)	0.194[b]
21–30 years	10 (15.2%)	9 (17%)	1 (7.7%)	
31–40 years	16 (24.2%)	11 (20.8%)	5 (38.5%)	
41–50 years	10 (15.2%)	10 (18.9%)	0 (0%)	
51–60 years	10 (15.2%)	9 (17%)	1 (7.7%)	
61–70 years	15 (22.7%)	10 (18.9%)	5 (38.5%)	
>70 years	2 (3%)	1 (1.9%)	1 (7.7%)	
Sex				
Male	39 (59.1%)	34 (64.2%)	5 (38.5%)	0.091[b]
Female	27 (40.9%)	19 (35.8%)	8 (61.5%)	
Clinical manifestation				
Paraparesis	27 (40.9%)	22 (41.5%)	5 (38.5%)	0.841[b]
Hemiparesis	18 (27.3%)	16 (30.2%)	2 (15.4%)	0.488[b]
Upper limbs tingling	9 (13.6%)	7 (13.2%)	2 (15.4%)	1.000[b]
Lower limbs tingling	10 (15.2%)	9 (17%)	1 (7.7%)	0.672[b]
Conus syndrome	2 (3%)	2 (3.8%)	0 (0%)	1.000[b]

N = Total number of patients in each group; qualitative data were expressed as a number (percentage).
[a] Mann–Whitney U test.
[b] Chi-square test; $p < 0.05$ is significant.

Table 2
Comparison between benign/borderline tumors and malignant tumors as regards conventional MRI findings.

Conventional MRI findings	All patients (*N* = 66)	Benign/low grade malignancies (*N* = 53)	High grade malignancies (*N* = 13)	*p*-value
Components				
Spinal cord enlargement	37 (56.1%)	32 (60.4%)	5 (38.5%)	0.154[b]
Spinal cord edema	9 (13.6%)	6 (11.3%)	3 (23.1%)	0.364[b]
Multiple spinal lesions	8 (12.1%)	5 (9.4%)	3 (23.1%)	0.185[b]
Brain involvement	5 (7.6%)	4 (7.5%)	1 (7.7%)	1.000[b]
Tumor size (mm)				
Mean ± SD	45.48 ± 15.90	30.03 ± 9.65	36.76 ± 16.98	0.419[a]
Median (range)	47 (18–72)	27 (19–60)	36 (15–66)	
⩽20 mm	10 (15.2%)	6 (11.3%)	4 (30.8%)	0.005[b]
21–30 mm	32 (48.5%)	31 (58.5%)	1 (7.7%)	
31–40 mm	11 (16.7%)	9 (17%)	2 (15.4%)	
41–50 mm	7 (10.6%)	3 (5.7%)	4 (30.8%)	
>50 mm	6 (9.1%)	4 (7.5%)	2 (15.4%)	
Tumor location				
Cervical	19 (28.8%)	17 (32.1%)	2 (15.4%)	0.060[b]
Thoracic	23 (34.8%)	19 (35.8%)	4 (30.8%)	
Cervicothoracic	9 (13.6%)	4 (7.5%)	5 (38.5%)	
Thoracolumbar	13 (19.7%)	11 (20.8%)	2 (15.4%)	
Conus	2 (3%)	2 (3.8%)	0 (0%)	
Tumor location				
Central	39 (59.1%)	36 (67.9%)	3 (23.1%)	0.003[b]
Eccentric	27 (40.9%)	17 (32.1%)	10 (76.9%)	
Margin				
Ill defined	62 (93.9%)	50 (94.3%)	12 (92.3%)	1.000[b]
Well defined	4 (6.1%)	3 (5.7%)	1 (7.7%)	
T1				
Hypointense	54 (81.8%)	45 (84.9%)	9 (69.2%)	0.182[b]
Isointense	10 (17.5%)	6 (11.3%)	4 (30.8%)	
Hyperintense	0 (0%)	2 (3.8%)	0 (0%)	
T2				
Hyperintense	55 (83.3%)	45 (84.9%)	10 (76.9%)	0.489[b]
Mixed	11 (16.7%)	8 (15.1%)	3 (23.1%)	
Pattern of enhancement				
No enhancement	3 (4.5%)	2 (3.8%)	1 (7.7%)	0.009[b]
Marginal	1 (1.5%)	1 (1.9%)	0 (0%)	
Focal	21 (31.8%)	12 (22.6%)	9 (69.2%)	
Diffuse	41 (62.1%)	38 (71.7%)	3 (23.1%)	
Homogeneity of contrast				
No enhancement	3 (4.5%)	2 (3.8%)	1 (7.7%)	0.004[b]
Homogenous	52 (78.8%)	46 (86.8%)	6 (46.2%)	
Heterogenous	11 (16.7%)	5 (9.4%)	6 (46.2%)	
Special findings				
Intratumoral cysts	3 (4.5%)	3 (5.7%)	0 (0%)	1.000[b]
Non-tumoral cyst	6 (9.1%)	5 (9.4%)	1 (7.7%)	1.000[b]
Cap sign	2 (3%)	0 (0%)	2 (15.4%)	0.036[b]
Hemorrhage	4 (6.1%)	3 (5.7%)	1 (7.7%)	1.000[b]
Syringomyelia	35 (53%)	32 (60.4%)	3 (23.1%)	0.016[b]

N = Total number of patients in each group; qualitative data were expressed as a number (percentage).
[a] Mann–Whitney U test.
[b] Chi-square test; $p < 0.05$ is significant.

value of s1000, and calculated mean apparent diffusion coefficient (ADC value).

3- Confirmatory work up: Histopathological confirmation.
4- Statistical analysis.

Continuous variables were expressed as the mean ± SD and median (Range), and the categorical variables were expressed as a number (percentage). Continuous variables were checked for normality by using Shapiro–Wilk test. Mann–Whitney U test was used to compare between two groups of non-normally distributed data. Kruskal–Wallis H test was used to compare between more than two groups of non-normally distributed data. Percent of categorical variables were compared using the Chi-square test or Fisher's exact test when appropriate. All tests were two sided with $p < 0.05$ which was considered statistically

significant. All data were analyzed using SPSS 22.0 for windows (SPSS Inc., Chicago, IL, USA).

4. Results

This study included 66 adult consecutive patients (39 male and 27 female) with intramedullary SOL tumor (IMSCT). The patients mean age was 45.48 ± 15.90 (18–72 y) (Table 1). Histopathological classification to benign/low grade malignancy group was in 53 patients and high grade malignancy group in 13 patients. No statistically significant difference between both groups regarding the patient age or their clinical presentation (Table 1).

Histological diagnosis was performed for all cases, biopsy in 4 patients (6.1%), partial excision in 53 patients (80.3%) and gross total excision in 9 patients (13.6%) (Table 2). Benign IMSC masses were in 2 patients (3%), one case was cavernoma (1.5%), and the other was dermoid cyst (1.5%). Low grade tumors (I, II) were found in 51 patients (77.2%), including ependymoma which was the most frequent in 28 (42.2%) patients (WHO grade II), and 5 (7.6%) patients grade I myopapillary type, one patient with grade I subependymoma (1.5%) and only one patient with an ependymoma had undergone a previous resection. Pleomorphic xanthoastrocytoma WHO Grade I was found in 5 patients (7.6%) and Astrocytoma (WHO Grade II) in 4 patients (6.1%). High grade tumors (grade III) were found in 6 patients (9.4%) as follows: anaplastic ependymoma in 4 patients (6.4%) and anaplastic astrocytoma in 2 patients (3%). Other malignant SC lesions were metastatic carcinoma in 5 patients (7.6%) and lymphoma in 2 patients (3%).

Table 3
Comparison between different tumors of spinal cord as regards conventional MRI findings.

Conventional MRI findings	All patients (*N* = 66)	Benign (*N* = 2)	Low grade tumors (*N* = 51)	High grade gliomas (*N* = 6)	Lymphoma (*N* = 2)	Spinal cord metastasis (*N* = 5)
Components						
Spinal cord enlargement	37 (56.1%)	0 (0%)	32 (62.7%)	2 (33.3%)	1 (50%)	2 (40%)
Spinal cord edema	9 (13.6%)	0 (0%)	6 (11.8%)	2 (33.3%)	0 (0%)	1 (20%)
Multiple spinal lesions	8 (12.1%)	0 (0%)	5 (9.8%)	1 (16.7%)	1 (50%)	1 (20%)
Brain involvement	5 (7.6%)	0 (0%)	4 (7.8%)	1 (16.7%)	0 (0%)	0 (0%)
Tumor size (mm)						
Mean ± SD	45.5 ± 15.9	29.5 ± 7.8	30.1 ± 9.8	47.8 ± 12.2	49 ± 1.4	18.6 ± 2.9
Median (range)	47 (18–72)	29.5 (24–35)	27 (19–60)	47.5 (34–66)	49 (48–50)	18 (15–23)
⩽20 mm	10 (15.2%)	0 (0%)	6 (11.8%)	0 (0%)	0 (0%)	4 (80%)
21–30 mm	32 (48.5%)	1 (50%)	30 (58.8%)	0 (0%)	0 (0%)	1 (20%)
31–40 mm	11 (16.7%)	1 (50%)	8 (15.7%)	2 (33.3%)	0 (0%)	0 (0%)
41–50 mm	7 (10.6%)	0 (0%)	3 (5.9%)	2 (33.3%)	2 (100%)	0 (0%)
>50 mm	6 (9.1%)	0 (0%)	4 (7.8%)	2 (33.3%)	0 (0%)	0 (0%)
Tumor location						
Cervical	19 (28.8%)	0 (0%)	17 (33.3%)	2 (33.3%)	0 (0%)	0 (0%)
Thoracic	23 (34.8%)	0 (0%)	19 (37.3%)	4 (66.7%)	0 (0%)	0 (0%)
Cervicothoracic	9 (13.6%)	0 (0%)	4 (7.8%)	0 (0%)	2 (100%)	3 (60%)
Thoracolumbar	13 (19.7%)	1 (50%)	10 (19.6%)	0 (0%)	0 (0%)	2 (40%)
Conus	2 (3%)	1 (50%)	1 (2%)	0 (0%)	0 (0%)	0 (0%)
Tumor location						
Central	39 (59.1%)	0 (0%)	36 (70.6%)	2 (33.3%)	0 (0%)	1 (20%)
Eccentric	27 (40.9%)	2 (100%)	15 (29.4%)	4 (66.7%)	2 (100%)	4 (80%)
Margin						
Ill defined	62 (93.9%)	2 (100%)	48 (94.1%)	6 (100%)	2 (100%)	4 (80%)
Well defined	4 (6.1%)	0 (0%)	3 (5.9%)	0 (0%)	0 (0%)	1 (20%)
T1						
Hypointense	54 (81.8%)	0 (0%)	45 (88.2%)	2 (33.3%)	2 (100%)	5 (100%)
Isointense	10 (17.5%)	0 (0%)	6 (11.8%)	4 (66.7%)	0 (0%)	0 (0%)
Hyperintense	0 (0%)	2 (100%)	0 (0%)	0 (0%)	0 (0%)	0 (0%)
T2						
Hyperintense	55 (83.3%)	0 (0%)	45 (88.2%)	3 (50%)	2 (100%)	5 (100%)
Mixed	11 (16.7%)	2 (100%)	6 (11.8%)	3 (50%)	0 (0%)	0 (0%)
Pattern of enhancement						
No enhancement	3 (4.5%)	2 (100%)	0 (0%)	0 (0%)	1 (50%)	0 (0%)
Marginal	1 (1.5%)	0 (0%)	1 (2%)	0 (0%)	0 (0%)	0 (0%)
Focal	21 (31.8%)	0 (0%)	12 (23.5%)	3 (50%)	1 (50%)	5 (100%)
Diffuse	41 (62.1%)	0 (0%)	38 (74.5%)	3 (50%)	0 (0%)	0 (0%)
Homogeneity of contrast						
No enhancement	3 (4.5%)	2 (100%)	0 (0%)	0 (0%)	1 (50%)	0 (0%)
Homogenous	52 (78.8%)	0 (0%)	46 (90.2%)	2 (33.3%)	0 (0%)	4 (80%)
Heterogenous	11 (16.7%)	0 (0%)	5 (9.8%)	4 (66.7%)	1 (50%)	1 (20%)

There was a statistically significant difference between the two groups regarding the tumor location and enhancement pattern (Table 2). Analysis of conventional MRI findings of the intramedullary spinal masses groups is summarized in Table 3.

Regarding low grade IMSC tumors (grades I and II) ependymomas (Fig. 1) and astrocytomas, their ADC mean values ranged from 1.27–1.81 $\times 10^{-3}$ mm^2/sec and ranged from 0.1 to 1.90 $\times 10^{-3}$ mm^2/sec, respectively (Table 4). One of the low grade ependymomas had low ADC value (1.04–1.2 $\times 10^{-3}$ mm^2/sec) denoting restricted diffusion which was correlated with histopathological analysis to be myopapillary type of the ependymoma with rich mucin contents (Fig. 2). In patients with hemangioblastoma (Fig. 3), the ADC ranged from 1 to 2.1 $\times 10^{-3}$ mm^2/sec (Table 3).

High grade IMSC tumors, were showing restricted diffusion with low ADC value ranging from 0.6 to

Table 4
Comparison between different tumors of spinal cord as regards diffusion MRI findings.

Diffusion MRI findings	Benign (N = 2)	Low grade tumors (N = 51)	High grade gliomas (N = 6)	Lymphoma (N = 2)	Spinal cord metastasis (N = 5)	p-value
Signal intensity of SC masses in DWIs at b value of s1000						
Hypointense	1 (50%)	48 (94.1%)	1 (16.7%)	0 (0%)	0 (0%)	<0.001[b]
Hyperintense	1 (50%)	3 (5.9%)	5 (83.3%)	2 (100%)	5 (100%)	
ADC for solid component ($\times 10^{-3}$ mm^2/sec)						
Mean ± SD	1.10 ± 0.42	1.27 ± 0.26	1.08 ± 0.43	0.60 ± 0.0	0.78 ± 0.37	0.020[a]
Median (range)	1.10 (0.80–1.40)	1.30 (0.60–1.90)	1.05 (0.6–0.9)		0.70 (0.40–1.01)	

N = Total number of patients in each group; qualitative data were expressed as a number (percentage).
[a] Kruskal–Wallis H test.
[b] Chi-square test; $p < 0.05$ is significant.

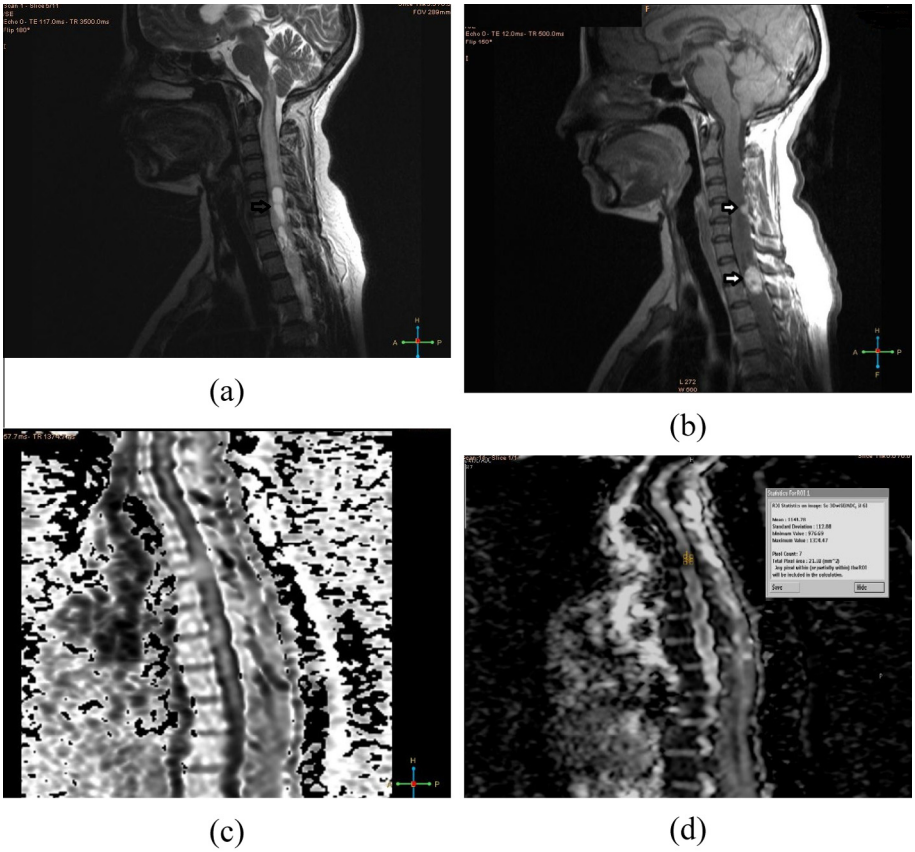

Fig. 1. 30-years-old female presented with sever neck pain and tingling. Sagittal T2-WI (A) shows a heterogeneous cystic and solid mass expanding the cord in the cervical and upper dorsal regions (arrow). Sagittal post-Gadolinium enhanced T1-weighted image (B) shows multiple enhanced portion (white arrow). DWI (C) and ADC (D) of the enhancing portion show hypointense and iso ADC (1.1 $\times 10^{-3}$ mm^2/sec) respectively. The findings of conventional MRI with DWI data, the case was diagnosed as ependymoma (low grade).

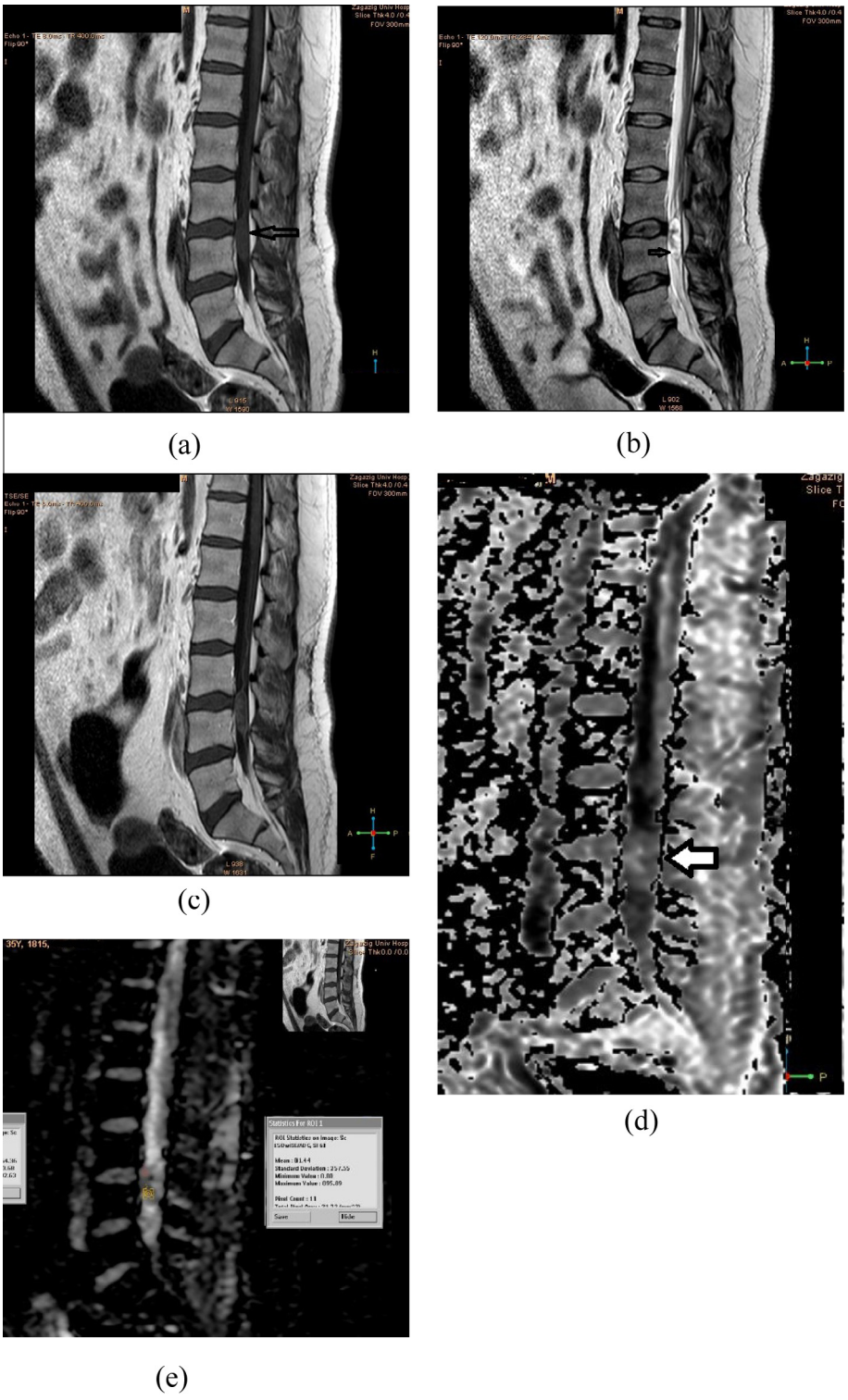

Fig. 2. 35-years-old male patient presented with low back pain since 4 months. (A) Sagittal T1WI shows heterogeneous isointense well defined oval shaped lesion (arrow) is seen at the distal part of the cord at the filum terminalis. (B) Sagittal T2WI shows heterogeneous hyper intensity of the lesion (arrow). (C) Sagittal post contrast image shows mild heterogeneous enhancement. (D) Sagittal DWI showed isointensity with central high signal area denoting restricted diffusion. (E) ADC map shows hyperintensity of the lesion denoting restricted diffusion. ADC value was 0.8×10^{-3} mm^2/sec. The lesion has DWI readings suggestive of restricted diffusion. The findings of conventional MRI with DWI data, the case was diagnosed as myxopapillary ependymoma (low grade).

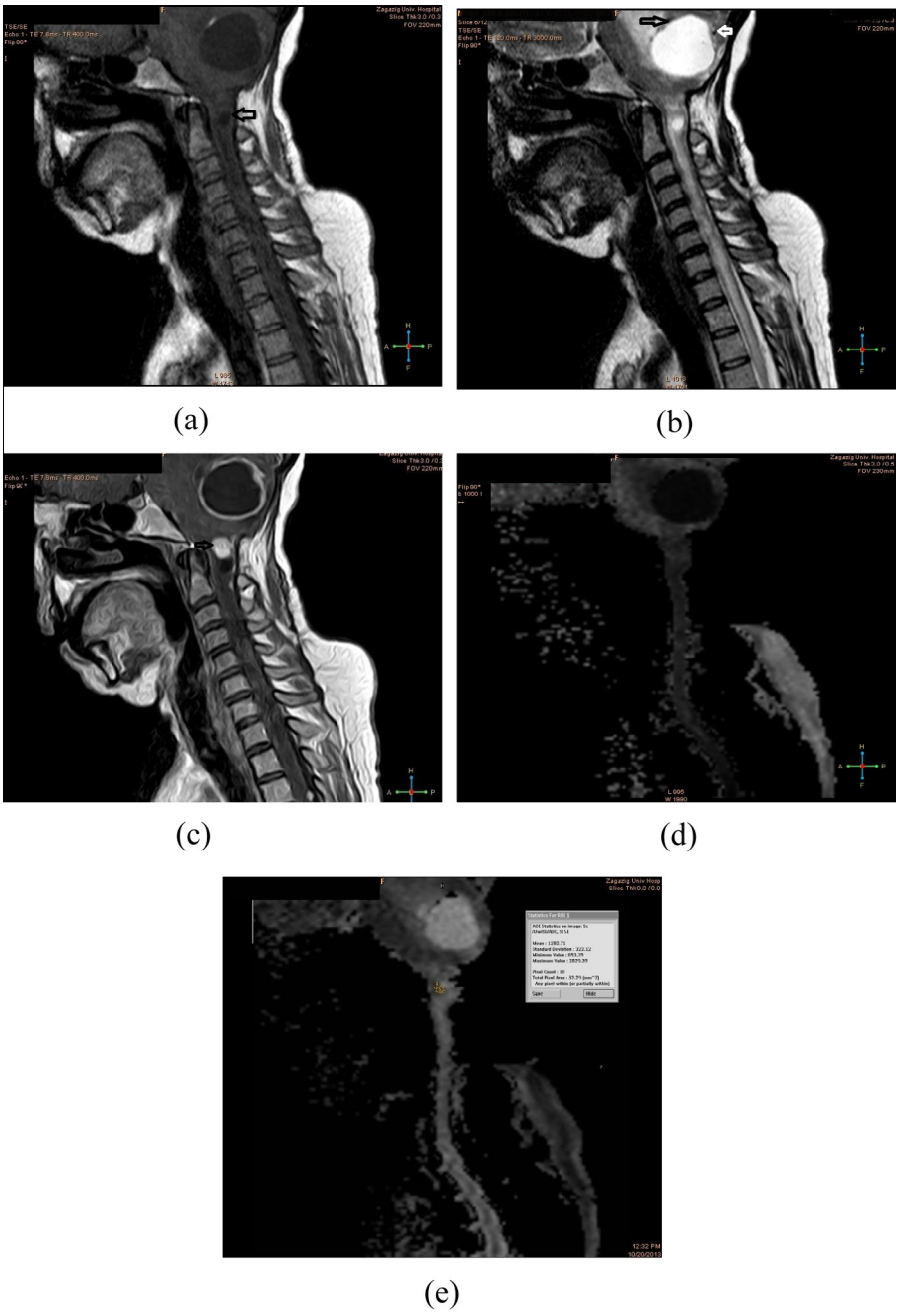

Fig. 3. 43-years-old female patient presented with three year history of severe headache, dizziness, unsteadiness, and tingling in upper limbs. Sagittal T1-WI (A), sagittal T2 WI (B) and sagittal T1WI post contrast (C) image show a large, well-demarcated cystic cerebellar and upper cervical intramedullary (arrow) cord lesions tumor opposite C 2 level. Homogenous hypo-intense solid nodule inside each cyst is noted and these nodules show intense and homogeneous enhancement (arrow in C). Vascular flow voids in and around the tumor (arrows), proved to be dilated veins at surgery. Hydrocephalic changes by the cerebellar mass and syringomyelia noted in the cervical cord. DWI (D) and ADC (E) are showing no restricted diffusion of the lesions, solid and contrast-enhancing portions appeared low signal on DWI. The ADC was increased (1.2×10^{-3} mm^2/sec). The findings of conventional MRI with DWI data, the case was diagnosed as low grade hemangioblastomas (Von Hipple-Lindau syndrome).

0.9×10^{-3} mm^2/sec (Fig. 4). Also low ADC values in other SC malignant infiltrations either by lymphoma or by metastatic deposits were as follows: 0.6×10^{-3} mm^2/sec and 0.40–1.01 $\times 10^{-3}$ mm^2/sec respectively (Table 4).

Only one patient presented with cavernoma (1.5%) which is a benign vascular malformation, and the ADC ranged from 1.2 to 1.4×10^{-3} mm^2/sec, while the other benign SC mass was epidermoid cyst with restricted

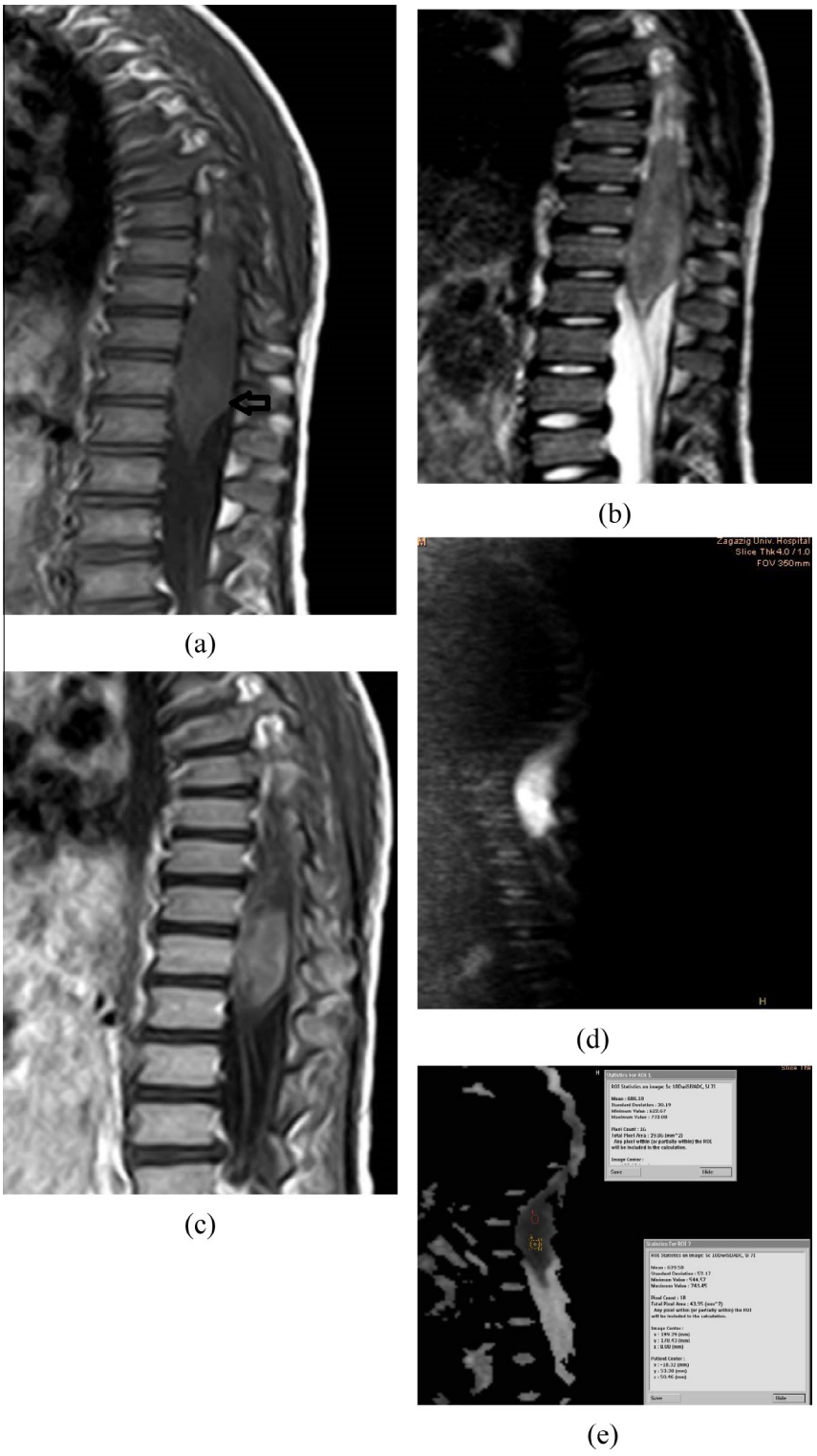

Fig. 4. 20-years-old male patient presented with low back pain and lower limbs paraplegia since 4 months. (A) Sagittal T1WI showed heterogeneous isointense intramedullary eccentric expansile mass is seen at the level of D7 to D12 spinal cord region (arrow). (B) Sagittal T2 WI showed heterogeneous slight hyper intensity of the lesion. (C) Sagittal T1 post-contrast enhancement showed mild heterogeneous enhancement. (D) DWI showed hyperintensity of the lesion with central high signal area denoting restricted diffusion. (E) ADC map showed hypointensity of the lesion denoting restricted diffusion. ADC value was 0.63×10^{-3} mm^2/sec. The findings of conventional MRI with DWI data, the case was diagnosed as high grade astrocytoma.

Table 5
Comparison between benign/low grade tumors and malignant tumors as regards diffusion MRI findings.

Diffusion MRI findings	All patients ($N = 66$)	Benign/low grade malignancies ($N = 53$)	High grade malignancies ($N = 13$)	p-value
Signal intensity of SC masses in DWIs at b value of s1000				
Hypointense	50 (77.8%)	49 (92.5%)	1 (7.7%)	<0.001[b]
Hyperintense	16 (24.2%)	4 (7.5%)	12 (92.3%)	
ADC for solid component ($\times 10^{-3}$ mm^2/sec)				
Mean ± SD	1.19 ± 0.33	1.26 ± 0.27	0.89 ± 0.40	0.004[a]
Median (range)	1.30 (0.40–1.90)	1.30 (0.60–1.90)	0.70 (0.40–1.01)	

N = Total number of patients in each group; qualitative data were expressed as a number (percentage).
[a] Mann–Whitney U test.
[b] Chi-square test; $p < 0.05$ is significant.

diffusion (the ADC of 0.8×10^{-3} mm^2/sec). There was statistically significant difference between the benign/low grade IMSC masses and high grade IMSC tumors ($p < 0.001$). Calculated mean ADC values in the benign/low grade tumors were 1.26×10^{-3} mm^2/sec high compared to high grade tumors which were $0.89 \pm 0.40 \times 10^{-3}$ mm^2/sec (Table 5).

5. Discussion

Diffusion weighted image and apparent diffusion coefficient may be markers for hypercellularity, especially in tumors of the spinal cord [9]. In our study benign/low grade IMSC masses were detected in 53 of 66 (80%) patients with spinal symptoms, while the high grade, and other malignant IMSC masses were found in 13 of 66 (20%) patients. No statistically significant difference between both groups regarding the patient age or their clinical presentation.

In our study ependymoma was the most frequent pathology, and this is not surprising as we focused on the adult age group only. Similarly many authors had reported that, ependymomas are the most common tumor type, accounting for 40–60% of all intramedullary spinal tumors, with the mean age of presentation being 35–40 years [6,10].

Regarding the conventional MRI characterization, statistically significant difference between both groups regarding the location and pattern of enhancement as the high grade/malignant tumors were located in eccentric location and heterogeneously enhanced than low grad group ($p > .005$).

DWI signals and ADC values of neoplasms depend on the cellularity and extracellular matrix. Low grade astrocytoma usually shows high ADC due to the abundant extracellular matrix containing more free water. Ependymoma shows iso ADC and often contains hemorrhage. Hypercellular tumor with less extracellular matrix such as high grade glioma, intramedullary metastasis, and lymphoma can show restricted diffusion with low ADC [11–13].

In our results we found that the mean ADC of benign lesions was 1.26×10^{-3} mm^2/sec while the mean ADC of malignant lesions was 0.89×10^{-3} mm^2/sec and there was a statistical significant difference between the two groups.

Similarly Serifoglu et al. [14] that found the median ADC values of the malignant tumors and benign lesions of the spinal cord were 0.72×10^{-3} mm^2/sec (range, $0.39–1.51 \times 10^{-3}$ mm^2/sec) and 1.17×10^{-3} mm^2/sec (range, $0.52–2.38 \times 10^{-3}$ mm^2/sec), respectively. There was a significant difference between ADC values of benign and malignant lesions ($P < 0.001$), and the cutoff point differentiating malignant lesions from benign pathologies is 0.98×10^{-3} mm^2/sec.

Moreover, in our study there was statistically significant difference between high grade astrocytoma and ependymoma compared to lymphoma cases. The high degree of cellularity in lymphomas has been used to explain the low signal intensities on T2W MR Images.

Many authors observed restricted diffusion in lymphomas in the brain. The comparison of water diffusibility in lymphomas and high-grade astrocytomas revealed a significant difference in ADC between those two neoplastic lesions. The mean ADC for cerebral lymphomas and high-grade astrocytomas was reported to be 0.87×10^{-3} and 1.21×10^{-3} mm^2/sec, respectively [11,15], with the cellularity of the lymphomas also significantly higher than that of the astrocytomas. Using DWI for the assessment of brain tumors has shown that ADC measurements may help to differentiate low-grade gliomas from high-grade gliomas, metastases and lymphomas. Minimum ADC values for low-grade gliomas were significantly higher than those of other tumors [11].

In our study SC metastatic deposit cases had a restricted diffusion with the low ADC values, which ranged from 0.40 to 1.01×10^{-3} mm^2/sec. Other authors had reported, that cellularity of metastatic lesions depends on the primary tumor. Metastases had lower cellularity and high ADC values, whereas in a patient with prostate cancer, metastases with high cellularity and low ADC values were measured, similar to those of lymphomas and sarcoma [16].

6. Conclusion

DWI may be useful in providing information about tumors grading not available with conventional MR imaging in the evaluation of IMSC masses.

Conflict of interest

We declare that we have no conflict of interest.

References

[1] Fazekas F, Kapeller P. Diseases of the spinal cord. In: Greenberg JO, editor. Neuroimaging: a companion to adams and victors principles of neurology. New York: McGraw-Hill; 1999. p. 521–42.

[2] LeBihan D. Molecular diffusion nuclear magnetic resonance imaging. Magn Reson J 1991;7:1–30.

[3] Moseley M, Cohen Y, Mintorovich J, et al. Early detection of regional cerebral ischemia in cats: comparison of diffusion and T2-weighted MRI and spectroscopy. Magn Reson Meds 1990;14:330–46.

[4] Sara W, Francesco G. Intradural spinal tumors and their mimics: a review of radiographic features. Postgrad Med J 2013;89:457–69.

[5] Louis D, Ohgaki H, Wiestler O, Cavenee W, Burger PC, Jouvet A. The 2007 WHO classification of tumours of the central nervous system. Acta Neuropathol 2007;114(2):97–109.

[6] Kim S, Bak K, Kim D, Kang T. Primary intramedullary spinal sarcoma : a case report and review of the current literatures. J Korean Neurosurg Soc 2010 Nov;48(5):448–51.

[7] Wang Z, Sun J, Xie J, Li Z, Ma C, Liu B, et al. Comparative analysis on the diagnosis and treatments of multisegment intramedullary spinal cord tumors between the different age groups. Neurosurg Rev 2011. August 6.

[8] Setzer M, Murtagh R, Murtagh F, et al. Diffusion tensor imaging tractography in patients with intramedullary tumors: comparison with intraoperative findings and value for prediction of tumor resectability. J Neurosurg Spine 2010;13:371–80.

[9] Raul Gs, Rafael F, Ellen G, Stephan E, Walter J. Diffusion in spinal cord infarction demonstrated by magnetic resonance line scan diffusion imaging. Stroke J 2012;43:532–5.

[10] Kim D, Kim J, Choi S, Sohn C, Yun J, Kim C, et al. Differentiation between Intramedullary spinal ependymoma and astrocytoma: comparative MRI analysis. Clin Radiol 2014;69:29–35.

[11] Johnson B, Fram E, Johnson P, Jacobowitz R. The variable MR appearance of primary lymphoma of the central nervous system: comparison with histopathologic features. AJNR Am J Neuroradiol 1997;18:563–72.

[12] Rollin N, Guyotat J, Streichenberger N, Honnorat J, Tran Minh VA, Cotton F. Clinical relevance of diffusion and perfusion magnetic resonance imaging in assessing intra-axial brain tumors. Neuroradiology 2006;48:150–9.

[13] Kim J, Moritani T. MRI diagnosis of spinal cord lesions with emphasis on diffusion-weighted imaging: characteristic findings, differential diagnoses and imaging pitfalls. ECR 2012. <www.myESR.org>. Post no:C-1924.

[14] Serifoglu I, Oz II, Damar M, Tokgoz O, Yazgan O, Erdem Z. Diffusion-weighted imaging in the head and neck region: usefulness of apparent diffusion coefficient values for characterization of lesions. Diagn Interv Radiol 2015;21(3):208–14.

[15] Guo AC, Cummings TJ, Dash R, Provenzale J. Lymphomas and high-grade astrocytomas: comparison of water diffusibility and histologic characteristics. Radiology 2002;224:177–83.

[16] Yan Z, Yongbo H, Xixing W, Jun W. Intramedullary spinal cord metastasis detected with whole body diffusion-weighted imaging. Neuorolgy India 2013;61–5:555–6.